An Autumn Stroll Among Random Tilings

At Low Temperatures With Local Rules

Léo Gayral

28/09/2021, Journée ANR DIMERS

IMT, Université Toulouse III Paul Sabatier

Physical Motivation

Quasicrystals

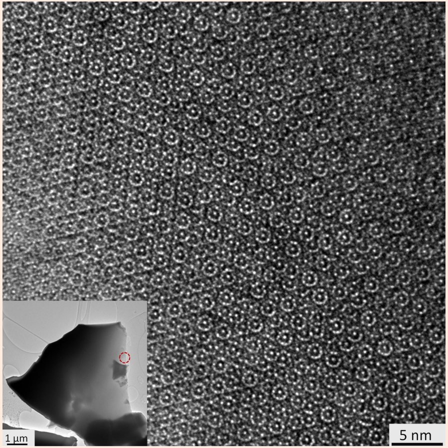

Figure 1: HRTEM image of a natural $Al_{71}Ni_{25}Fe_5$ Decagonite quasicrystal with plane decagonal rotational symmetry [Bindi et al., 2015, Figure 5].

Aperiodic Tilings

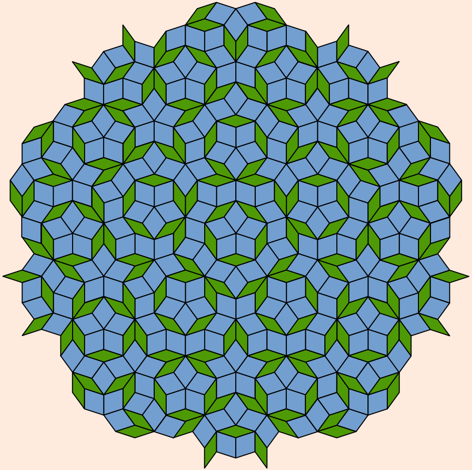

Figure 2: The Penrose tiling has a pentagonal rotational symmetry.

Gibbs Measures and Local Rules

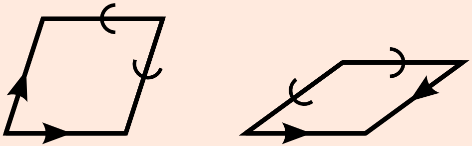

Figure 3: Matching arrows on the edges of the rhombuses forces the Penrose tiling.

Random Dimers With Local Rules

A Random Dimer Model

Dimer Tilings

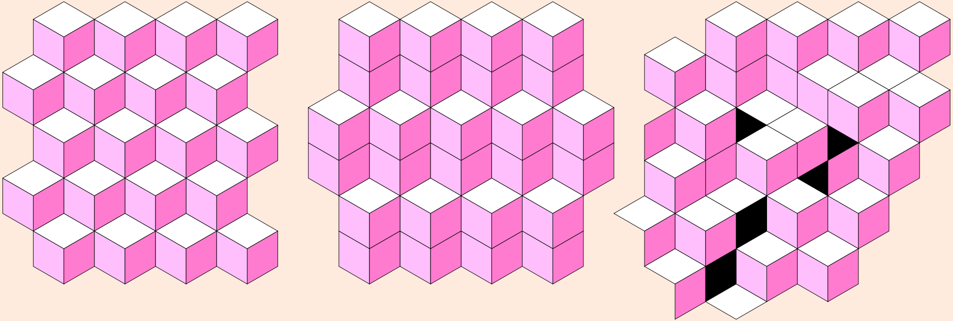

Figure 4: Tiling examples.

Height Function

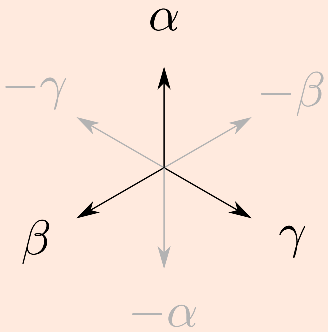

Figure 5: General weighted arrows.

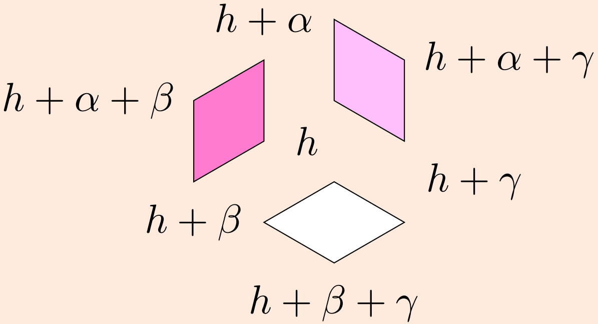

Figure 6: Relative heights of the vertices of a tile.

Height Function

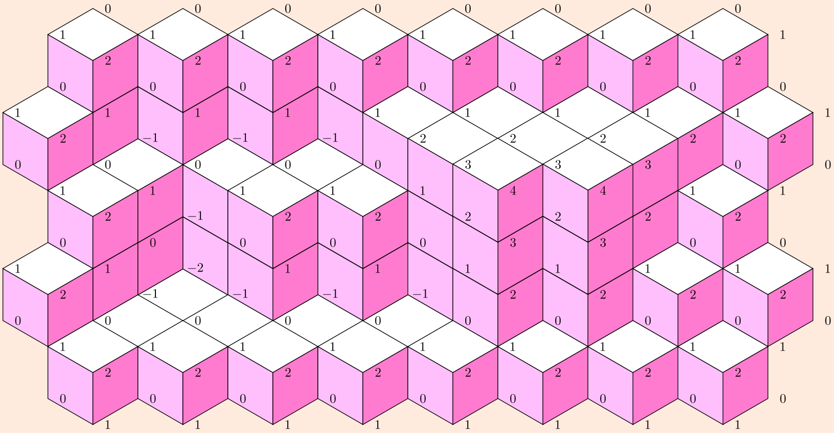

Figure 7: Height function on the vertices with $\alpha = \beta = \gamma = 1$.

Local Rules Through Forbidden Patterns

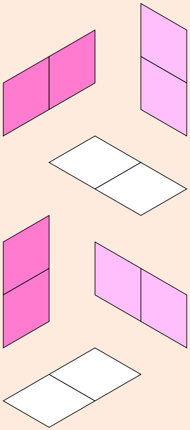

Figure 8: Forbidden patterns.

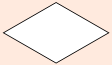

Figure 9: Locally admissible tiling.

Local Rules Through Forbidden Patterns

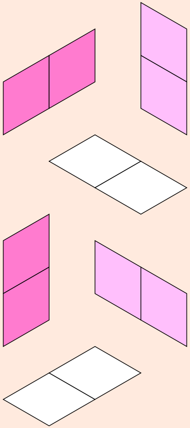

Figure 8: Forbidden patterns.

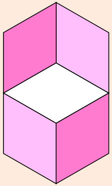

Figure 9: Locally admissible tiling.

Local Rules Through Forbidden Patterns

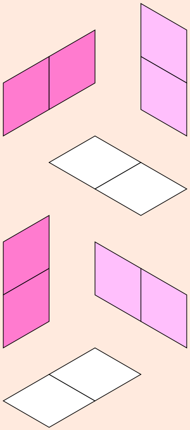

Figure 8: Forbidden patterns.

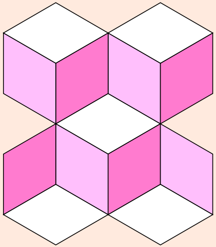

Figure 9: Locally admissible tiling.

Local Rules Through Forbidden Patterns

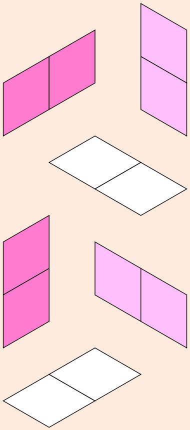

Figure 8: Forbidden patterns.

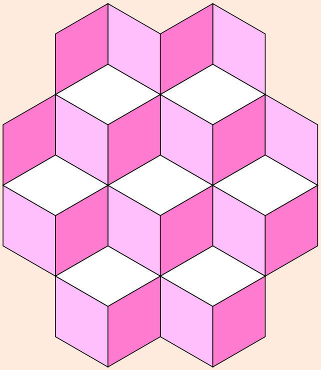

Figure 9: Locally admissible tiling.

Associated Gibbs Measure

Definition

Consider Λ a tileable, simply connected, compact domain,
and $E(\eta)$ the number of forbidden patterns in a tiling η of Λ.

We define $\mu_{\Lambda,\beta}(\eta) := \frac{1}{Z_{\Lambda,\beta}} \exp\left(-\beta \times E(\eta)\right)$ the Gibbs measure at inverse temperature β.

Associated Gibbs Measure

Definition

Consider Λ a tileable, simply connected, compact domain,
and $E(\eta)$ the number of forbidden patterns in a tiling η of Λ.

We define $\mu_{\Lambda,\beta}(\eta) := \frac{1}{Z_{\Lambda,\beta}} \exp\left(-\beta \times E(\eta)\right)$ the Gibbs measure at inverse temperature β.

Can we control $\mathbb{E}_{\Lambda,\beta}[\,|H(x)|\,]$, with H the height of a vertex $x \in \Lambda$?

Random Dimers With Local Rules

Peierls Argument for Random Dimers

Hexagonal Contours Induced by Forbidden Patterns

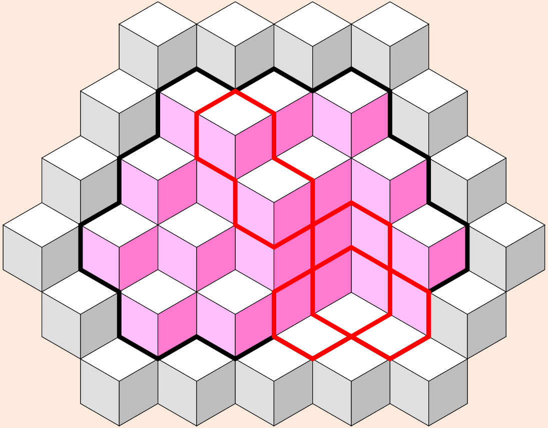

Figure 10: Rule violations can be decomposed into a family of cycles.

Hexagonal Contours Induced by Forbidden Patterns

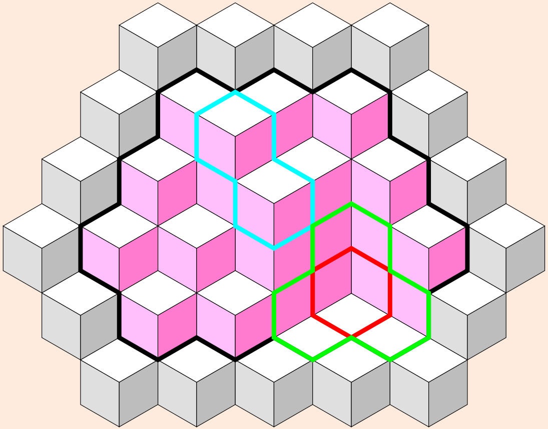

Figure 10: Rule violations can be decomposed into a family of cycles.

Relative Height and Number of Cycles

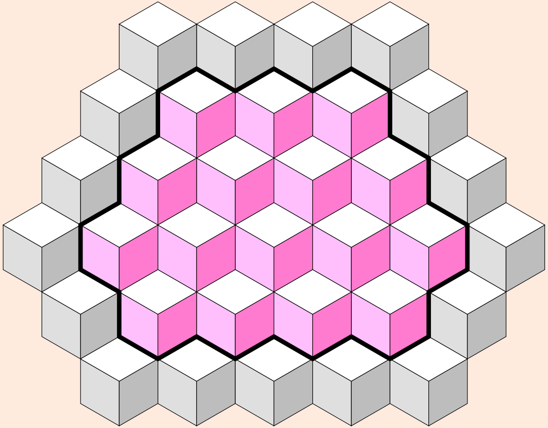

Figure 11: The number of cycles linearly impacts the height difference.

Relative Height and Number of Cycles

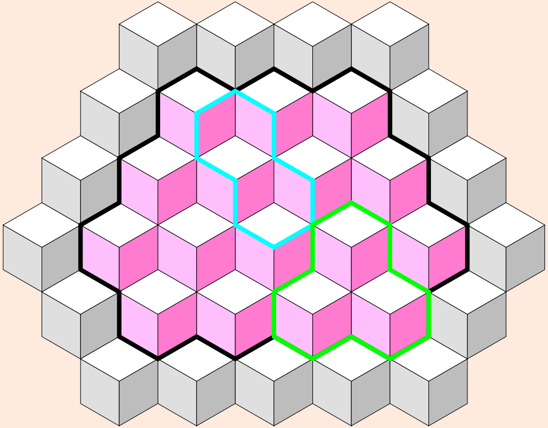

Figure 11: The number of cycles linearly impacts the height difference.

Relative Height and Number of Cycles

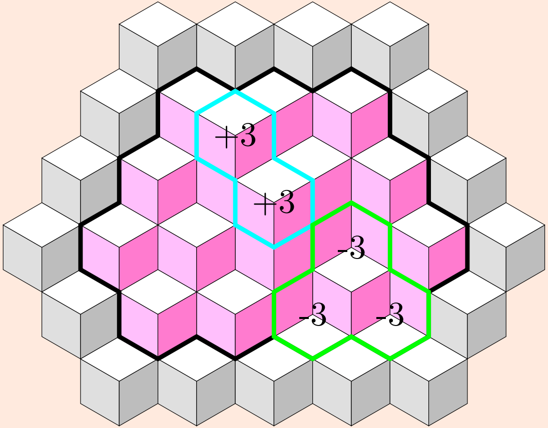

Figure 11: The number of cycles linearly impacts the height difference.

Relative Height and Number of Cycles

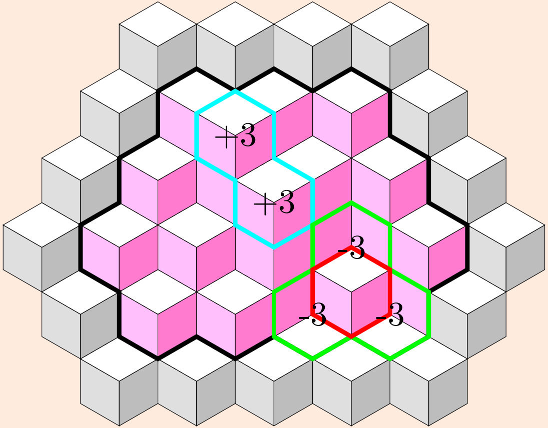

Figure 11: The number of cycles linearly impacts the height difference.

Relative Height and Number of Cycles

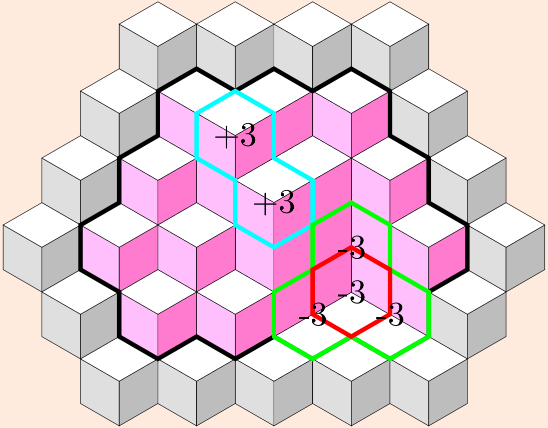

Figure 11: The number of cycles linearly impacts the height difference.

Relative Height and Number of Cycles

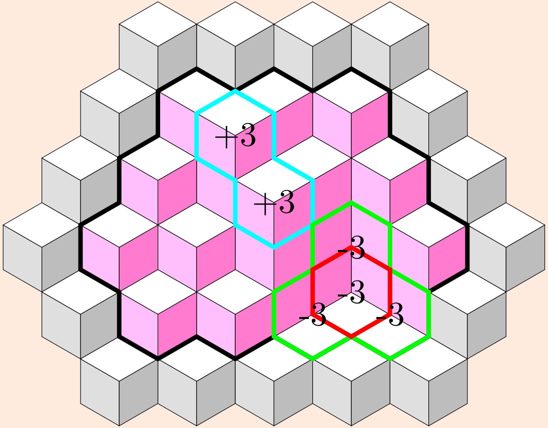

Figure 11: The number of cycles linearly impacts the height difference.

We have $|H - H_0| \leq 3T$, with H_0 the height without forbidden patterns, and T the number of cycles around a vertex.

Cycle Correction Decreases Energy

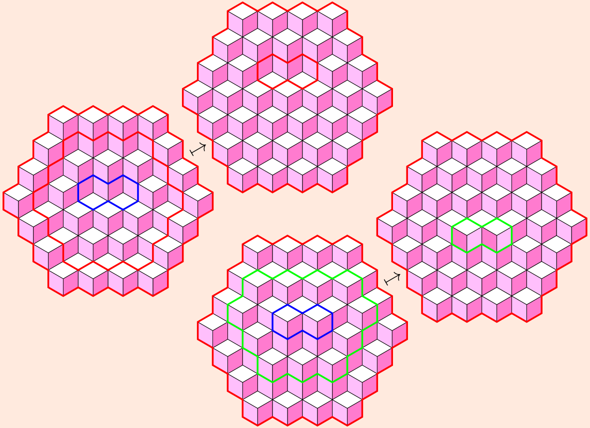

Figure 12: In both examples we correct the cycle *around* the small blue one.

If we obtain η' by correcting the cycle γ from η, then $E(\eta) = E(\eta') + |\gamma|$.

Peierls Argument

Theorem

We have $\mathbb{E}_\beta[T] \leq \exp\left(\frac{9e^{2\beta}}{2(e^\beta+2)^2} \times \frac{1}{(e^\beta-2)^2}\right) - 1 < \infty$ *when* $\beta > \ln(2)$.

Proof.

See Appendix 1. $\square$

It follows that $|H - H_0|$ stays bounded on average *on a given vertex.*

However, it is expected that $|H - H_0|$ isn't bounded and takes arbitrarily high values.

Peierls Argument

Theorem

We have $\mathbb{E}_\beta[T] \leq \exp\left(\frac{9e^{2\beta}}{2(e^\beta+2)^2} \times \frac{1}{(e^\beta-2)^2}\right) - 1 < \infty$ *when* $\beta > \ln(2)$.

Proof.

See Appendix 1. $\square$

It follows that $|H - H_0|$ stays bounded on average *on a given vertex.*

However, it is expected that $|H - H_0|$ isn't bounded and takes arbitrarily high values.

Could we prove that $H \notin L^1$ when β is small-enough?

Random Dimers With Local Rules

Generalisation of the Result

Key Ingredients for the Peierls Argument

We need a good notion of contours, such that:

- We have a relation between contours and the height, *e.g.* $H = O(T)$,
- We can injectively erase a contour while decreasing the energy, *e.g.* $E(\eta) \geq E(\eta') + O(|\gamma|)$.

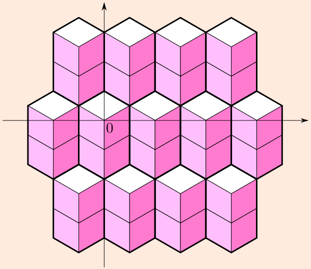

Figure 13: Periodic discrete surface corresponding to the plane $(2, 2, 1)^{\perp}$.

Forbidden Patterns Won't Define Cycles...

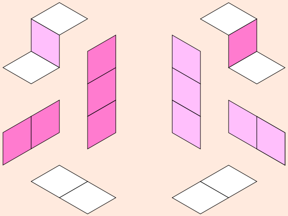

Figure 14: Forbidden patterns.

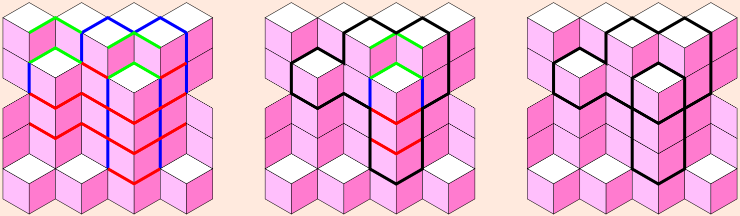

Figure 15: Empirical choice of contours.

Amidst a worldwide plague, my internship ended on this roadblock.

...But What If Contours Were Thick?

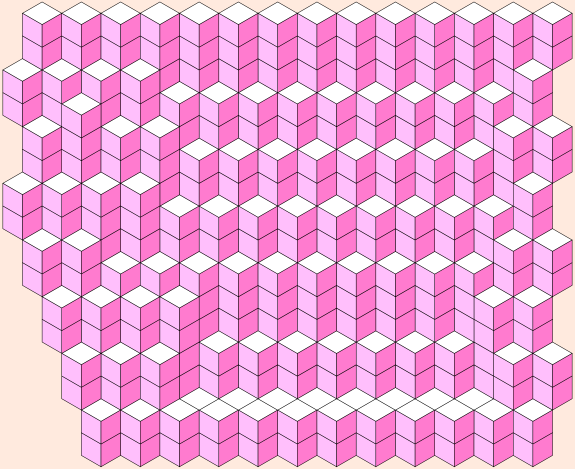

Figure 16: Here, instead of cycles made of edges,

...But What If Contours Were Thick?

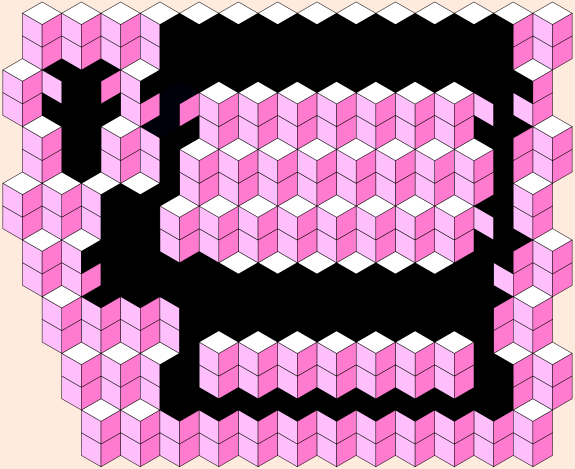

Figure 16: Here, instead of cycles made of edges, we define thick contours made of tiles.

Wang Tiles with Bernoulli Noise

General Framework

Subshifts of Finite Type

×	○	×	○	×	○	×	○	×	○	×	○	×
○	○	×	○	○	×	×	○	×	○	×	○	×
×	○	○	○	○	○	×	×	○	○	×	○	×
○	×	×	×	○	×	○	×	○	×	○	×	○
×	○	×	×	×	×	○	○	○	○	○	○	×
○	○	×	×	×	×	○	×	○	○	×	○	×
×	×	×	○	×	○	○	×	×	○	○	○	×
○	×	○	×	○	×	×	×	×	×	○	×	○

Figure 17: Example of configuration,

- Grid $\mathbb{Z}^2$.
- Alphabet $\mathcal{A} = \{\circ, \times\}$.

Subshifts of Finite Type

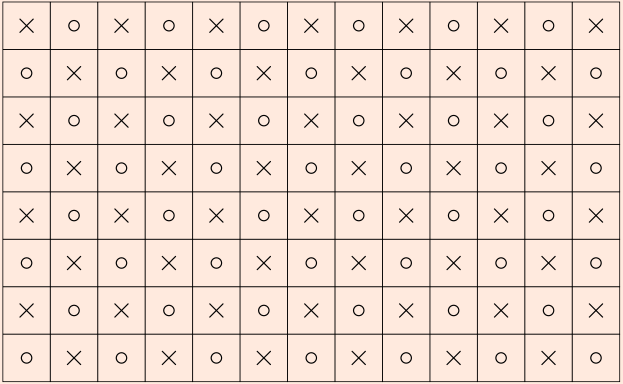

Figure 17: Example of configuration, without forbidden patterns.

- Grid $\mathbb{Z}^2$.
- Alphabet $\mathcal{A} = \{\circ, \times\}$.
- Forbidden patterns $\mathcal{F}$:

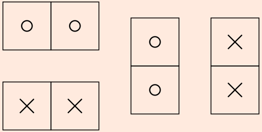

Subshifts of Finite Type

×	○	×	○	×	○	×	○	×	○	×	○	×
○	×	○	×	○	×	○	×	○	×	○	×	○
×	○	×	○	×	○	×	○	×	○	×	○	×
○	×	○	×	○	×	○	×	○	×	○	×	○
×	○	×	○	×	○	×	○	×	○	×	○	×
○	×	○	×	○	×	○	×	○	×	○	×	○
×	○	×	○	×	○	×	○	×	○	×	○	×
○	×	○	×	○	×	○	×	○	×	○	×	○

Figure 17: Example of configuration, without forbidden patterns.

- Grid $\mathbb{Z}^2$.
- Alphabet $\mathcal{A} = \{\circ, \times\}$.
- Forbidden patterns $\mathcal{F}$:

○	○

×	×

○
○

×
×

The SFT is the space $\Omega_{\mathcal{F}} \subset \mathcal{A}^{\mathbb{Z}^d}$ of such configurations.

Denote $\mathcal{M}_{\mathcal{F}}$ the σ-invariant measures on $\Omega_{\mathcal{F}}$.

Clair-Obscur Framework

- Inject $\mathcal{A} \hookrightarrow \widetilde{\mathcal{A}} = \mathcal{A} \times \{0,1\}$.

×	○	×	○	×	○	×	○	×	○	×	○	×
○	○	×	○	○	×	×	○	×	○	×	○	×
×	○	○	○	○	○	×	×	○	○	×	○	×
○	×	×	×	○	×	○	×	○	×	○	×	○
×	○	×	×	×	×	○	○	○	○	○	○	×
○	○	×	×	×	×	○	×	○	○	×	○	×
×	×	×	○	×	○	○	×	×	○	○	○	×
○	×	○	×	○	×	×	×	×	×	○	×	○

Figure 18: Configuration,

Clair-Obscur Framework

- Inject $\mathcal{A} \hookrightarrow \widetilde{\mathcal{A}} = \mathcal{A} \times \{0,1\}$.
- Identify $\mathcal{F} \cong \widetilde{\mathcal{F}} = \mathcal{F} \times \{0\}$.

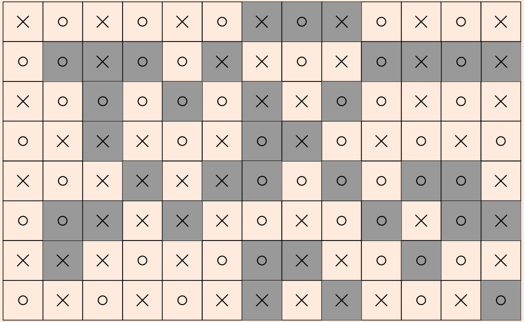

Figure 18: Configuration, now with obscured cells.

Clair-Obscur Framework

- Inject $\mathcal{A} \hookrightarrow \widetilde{\mathcal{A}} = \mathcal{A} \times \{0,1\}$.
- Identify $\mathcal{F} \cong \widetilde{\mathcal{F}} = \mathcal{F} \times \{0\}$.
- Denote $\widetilde{\mathcal{M}^{\mathcal{B}}_{\mathcal{F}}}(\varepsilon) \subset \mathcal{M}_{\widetilde{\mathcal{F}}}$ the measures with $\mathcal{B}(\varepsilon)^{\otimes \mathbb{Z}^d}$ Bernoulli noise.

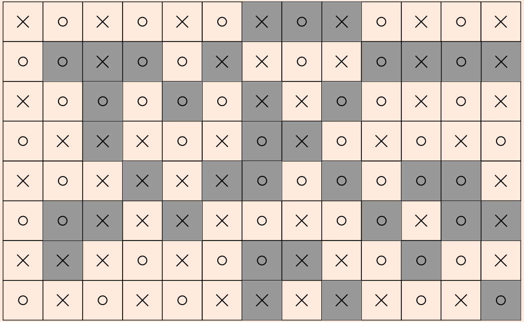

Figure 18: Configuration, now with obscured cells.

Clair-Obscur Framework

- Inject $\mathcal{A} \hookrightarrow \widetilde{\mathcal{A}} = \mathcal{A} \times \{0,1\}$.
- Identify $\mathcal{F} \cong \widetilde{\mathcal{F}} = \mathcal{F} \times \{0\}$.
- Denote $\widetilde{\mathcal{M}^{\mathcal{B}}_{\mathcal{F}}}(\varepsilon) \subset \mathcal{M}_{\widetilde{\mathcal{F}}}$ the measures with $\mathcal{B}(\varepsilon)^{\otimes \mathbb{Z}^d}$ Bernoulli noise.
- The set $\widetilde{\mathcal{M}^{\mathcal{B}}_{\mathcal{F}}}(\varepsilon)$ is weak-* closed, and $\bigcap_{\varepsilon>0} \widetilde{\mathcal{M}^{\mathcal{B}}_{\mathcal{F}}}(\varepsilon) = \mathcal{M}_{\mathcal{F}}$.

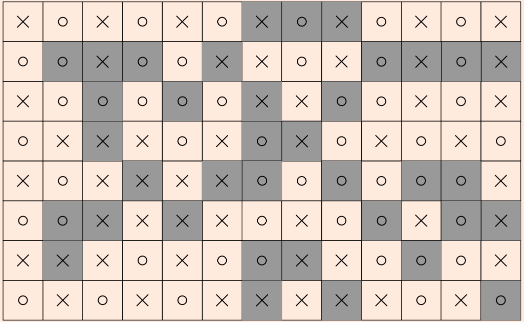

Figure 18: Configuration, now with obscured cells.

Reminder (Weak-* Convergence)

We say that $\mu_n \xrightarrow{*} \mu$ *when* $\mu_n([w]) \to \mu([w])$ *for any finite pattern* w.

Besicovitch Distance

x

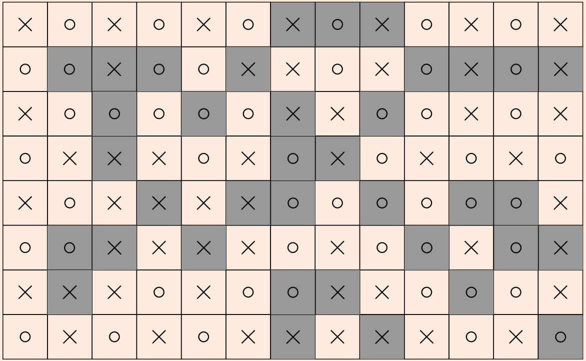

Figure 19: Frequency of differences between x and y.

Finite Hamming distance:

$$d_{13\times 8}(x,\quad) = \frac{\quad}{13\times 8}$$

Besicovitch Distance

y

×	○	×	○	×	○	×	○	×	○	×	○	×
○	×	○	×	○	×	○	×	○	×	○	×	○
×	○	×	○	×	○	×	○	×	○	×	○	×
○	×	○	×	○	×	○	×	○	×	○	×	○
×	○	×	○	×	○	×	○	×	○	×	○	×
○	×	○	×	○	×	○	×	○	×	○	×	○
×	○	×	○	×	○	×	○	×	○	×	○	×
○	×	○	×	○	×	○	×	○	×	○	×	○

Figure 19: Frequency of differences between x and y.

Finite Hamming distance:

$$d_{13\times 8}(x,y) = \frac{}{13\times 8}$$

Besicovitch Distance

$x|y$

×	○	×	○	×	○	×	○	×	○	×	○	×
○	⊗	⊗	⊗	○	×	⊗	⊗	⊗	⊗	⊗	⊗	⊗
×	○	⊗	○	⊗	○	×	⊗	⊗	○	×	○	×
○	×	⊗	×	○	×	○	×	○	×	○	×	○
×	○	×	⊗	×	⊗	⊗	○	⊗	○	⊗	○	×
○	⊗	⊗	×	⊗	×	○	×	○	⊗	⊗	⊗	⊗
×	⊗	×	○	×	○	⊗	⊗	×	○	⊗	○	×
○	×	○	×	○	×	⊗	×	⊗	×	○	×	○

Figure 19: Frequency of differences between x and y.

Finite Hamming distance:

$$d_{13\times 8}(x,y) = \frac{33}{13\times 8} \approx 0.3$$

Besicovitch Distance

$x|y$

×	○	×	○	×	○	×	○	×	○	×	○	×
○	⊗	⊗	⊗	○	×	⊗	⊗	⊗	⊗	⊗	⊗	⊗
×	○	⊗	○	⊗	○	×	⊗	⊗	○	×	○	×
○	×	⊗	×	○	×	○	×	○	×	○	×	○
×	○	×	⊗	×	⊗	⊗	○	⊗	○	⊗	○	×
○	⊗	⊗	×	⊗	×	○	×	○	⊗	⊗	⊗	⊗
×	⊗	×	○	×	○	⊗	⊗	×	○	⊗	○	×
○	×	○	×	○	×	⊗	×	⊗	×	○	×	○

Figure 19: Frequency of differences between x and y.

Finite Hamming distance:

$$d_{13\times 8}(x,y) = \frac{33}{13\times 8} \approx 0.3$$

Hamming-Besicovitch pseudo-distance:

$$d_H = \limsup_{n\to\infty} d_{n\times n}$$

Besicovitch Distance

$x|y$

×	○	×	○	×	○	×	○	×	○	×	○	×
○	⊗	⊗	⊗	○	×	⊗	⊗	⊗	⊗	⊗	⊗	⊗
×	○	⊗	○	⊗	○	×	⊗	⊗	○	×	○	×
○	×	⊗	×	○	×	○	×	○	×	○	×	○
×	○	×	⊗	×	⊗	⊗	○	⊗	○	⊗	○	×
○	⊗	⊗	×	⊗	×	○	×	○	⊗	⊗	⊗	⊗
×	⊗	×	○	×	○	⊗	⊗	×	○	⊗	○	×
○	×	○	×	○	×	⊗	×	⊗	×	○	×	○

Figure 19: Frequency of differences between x and y.

Finite Hamming distance:

$$d_{13\times 8}(x,y) = \frac{33}{13\times 8} \approx 0.3$$

Hamming-Besicovitch pseudo-distance:

$$d_H = \limsup_{n\to\infty} d_{n\times n}$$

Besicovitch distance on σ-invariant measures:

$$d_B(\mu,\nu) = \inf_{\lambda \text{ a coupling}} \int d_H(x,y)\mathrm{d}\lambda(x,y)$$

Stability

The SFT $\Omega_{\mathcal{F}}$ is f-stable for d_B on Bernoulli noises if:

$$\forall \varepsilon > 0, \quad \sup_{\lambda \in \widetilde{\mathcal{M}_{\mathcal{F}}^{\mathcal{B}}}(\varepsilon)} d_B\left(\pi_1^*(\lambda), \mathcal{M}_{\mathcal{F}}\right) \leq f(\varepsilon).$$

Stability

The SFT $\Omega_{\mathcal{F}}$ is f-stable for d_B on Bernoulli noises if:

$$\forall \varepsilon > 0, \quad \sup_{\lambda \in \widetilde{\mathcal{M}_{\mathcal{F}}^{\mathcal{B}}}(\varepsilon)} d_B\left(\pi_1^*(\lambda), \mathcal{M}_{\mathcal{F}}\right) \leq f(\varepsilon).$$

Theorem [Gayral and Sablik, 2021, Corollary 3.15]

Stability is conjugacy-invariant.

Stability

The SFT $\Omega_{\mathcal{F}}$ is f-stable for d_B on Bernoulli noises if:

$$\forall \varepsilon > 0, \quad \sup_{\lambda \in \widetilde{\mathcal{M}_{\mathcal{F}}^{\mathcal{B}}}(\varepsilon)} d_B\left(\pi_1^*(\lambda), \mathcal{M}_{\mathcal{F}}\right) \leq f(\varepsilon).$$

Theorem [Gayral and Sablik, 2021, Corollary 3.15]

Stability is conjugacy-invariant.

What kind of (in)stability results can we expect from typical SFTs?

Wang Tiles with Bernoulli Noise

Stability of the Periodic Subshifts

1D Classification of the Stability

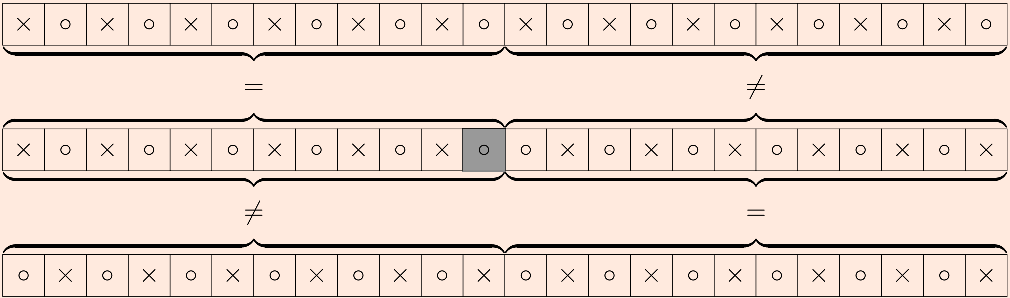

Figure 20: The noisy configuration is at Hamming distance $\frac{1}{2}$ of the clear ones.

1D Classification of the Stability

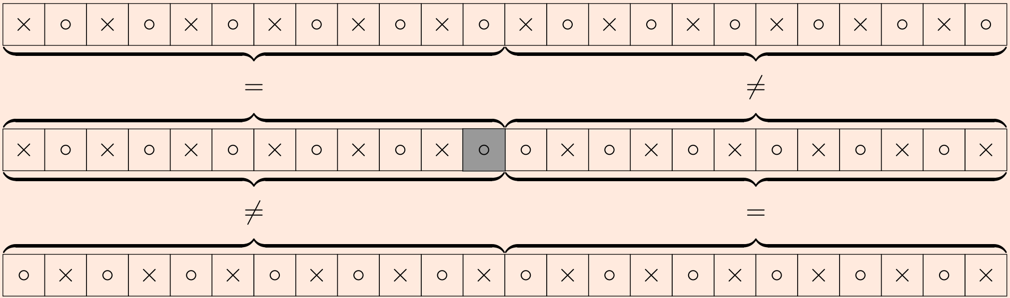

Figure 20: The noisy configuration is at Hamming distance $\frac{1}{2}$ of the clear ones.

Theorem [Gayral and Sablik, 2021, Theorem 4.8 and Theorem 4.9]

Consider $\Omega_{\mathcal{F}}$ a 1D SFT. Then $\Omega_{\mathcal{F}}$ is (linearly) stable on Bernoulli noises iff it is mixing.

Most notably, p-periodic SFTs (with $p \geq 2$) are unstable.

Periodic Tilings in Higher Dimensions

A SFT $\Omega_{\mathcal{F}}$ is (strongly) periodic if there exists an integer N such that any configuration is invariant for any translation in $(N\mathbb{Z})^d$.

Theorem [Gayral and Sablik, 2021, Theorem 5.7]

Consider $\Omega_{\mathcal{F}}$ a 2D+ periodic SFT.

Then $\Omega_{\mathcal{F}}$ is f-stable on Bernoulli noises, with linear speed $f(\varepsilon) = 2C^d_{c(\mathcal{F})}\varepsilon$.

Reconstruction Function

Lemma [Gayral and Sablik, 2021, Lemma 5.3]

Consider a 2D+ periodic SFT $\Omega_{\mathcal{F}}$.

There exists $c(\mathcal{F}) \geq \lceil \frac{N}{2} \rceil$ such that, for any connected cell window $I \subset \mathbb{Z}^d$, if $w \in \mathcal{A}^{I+B_c}$ is locally admissible, then $w|_I$ is globally admissible.

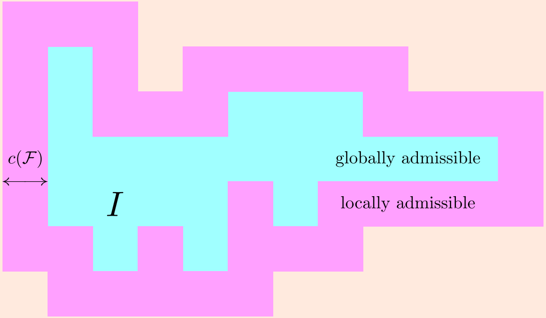

Figure 21: Here, the whole domain contains no forbidden pattern, but only the blue zone is guaranteed to be the restriction of an actual configuration.

Thickened Percolation

Consider $\varphi_n(b)_x = \max_{\|y-x\|_\infty \leq n} b_y$ for $b \in \{0,1\}^{\mathbb{Z}^d}$.

Starting from a site percolation ν, we obtain the n-thickened percolation $\varphi_n^*(\nu)$.

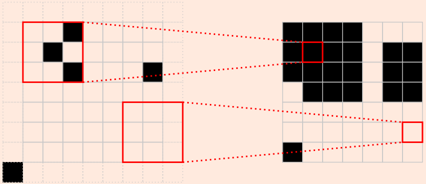

Figure 22: Illustration of the mapping φ_1.

Proposition [Gayral and Sablik, 2021, Proposition 5.6]

Consider $I \subset \mathbb{Z}^d$ the random infinite component of the n-thickened $\mathcal{B}(\varepsilon)^{\otimes \mathbb{Z}^d}$-percolation.

Then $C_n^d = 48(2n+1)^d$ is such that $\mathbb{P}(0 \notin I) \leq C_n^d \times \varepsilon$.

Wang Tiles with Bernoulli Noise

The Aperiodic Robinson Tiling

The (Enhanced) Robinson Tiling

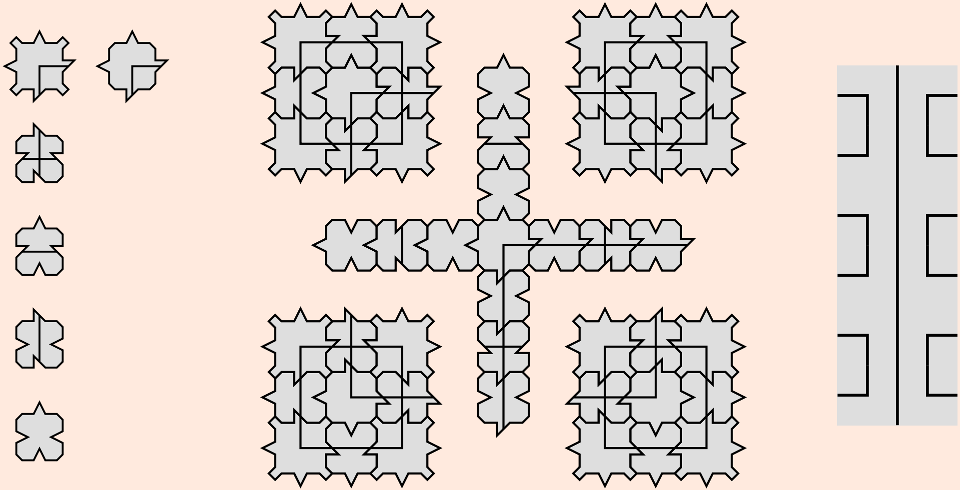

Figure 23: Tileset and hierarchical structure of the Robinson tiling,

The (Enhanced) Robinson Tiling

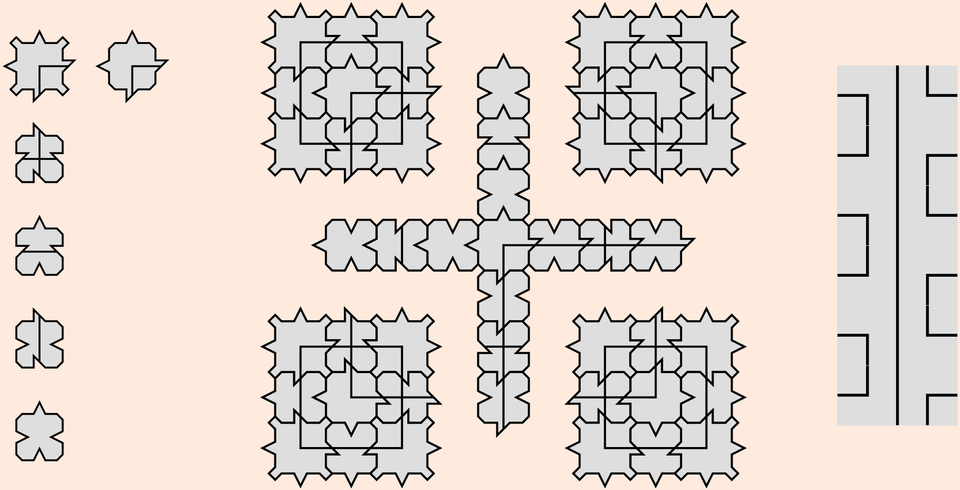

Figure 23: Tileset and hierarchical structure of the Robinson tiling,

The (Enhanced) Robinson Tiling

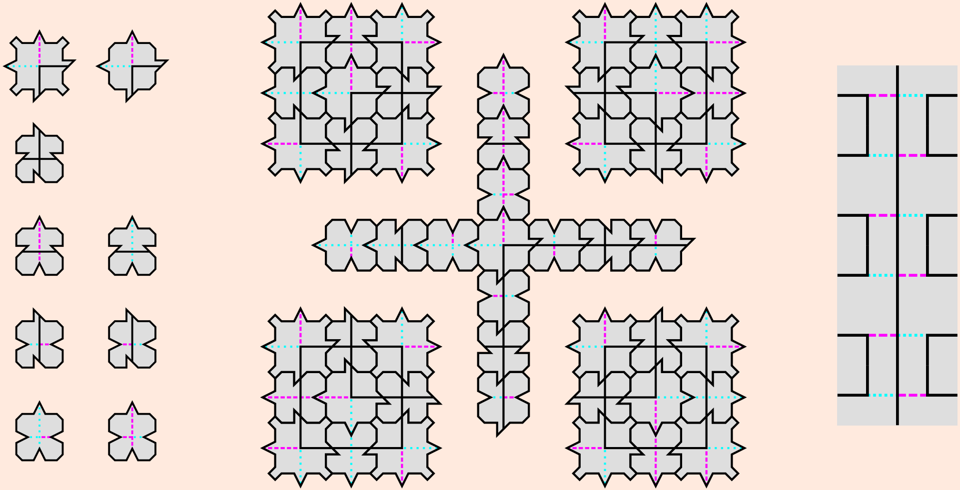

Figure 23: Tileset and hierarchical structure of the Robinson tiling, with strengthened local rules.

Reconstruction Function for the Enhanced Tiling

Proposition [Gayral and Sablik, 2021, Proposition 7.7]

For any scale $N \geq 2$, the constant $C_N = 2^N - 1$ is such that
for any integer n and any clear locally admissible pattern w on B_{n+C_N},
$w|_{B_n}$ is almost globally admissible, in the sense that up to a low-density grid,
$w|_{B_n}$ is made of well-aligned and well-oriented N-macro-tiles.

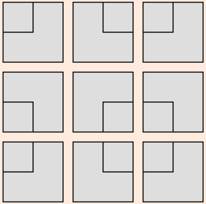

Figure 24: Family of well-aligned and well-oriented tiles.

Density of the Grid

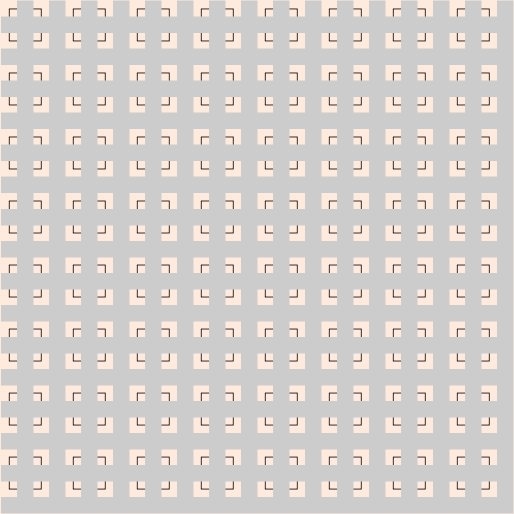

Figure 25: The density of the grid around N-macro-tiles goes to 0 as $N \to \infty$.

Density of the Grid

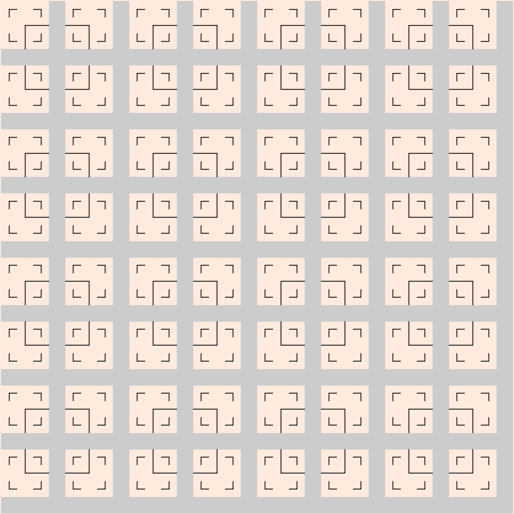

Figure 25: The density of the grid around N-macro-tiles goes to 0 as $N \to \infty$.

Density of the Grid

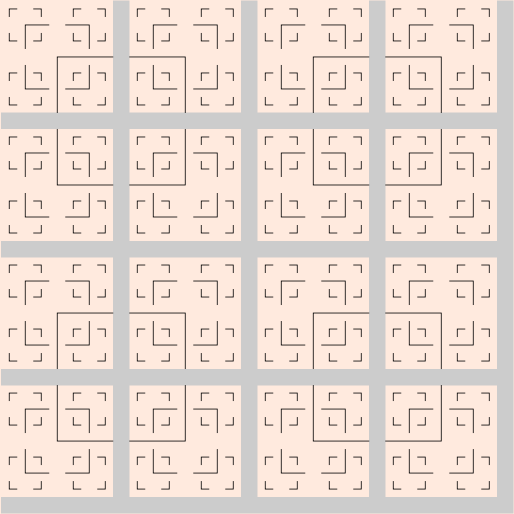

Figure 25: The density of the grid around N-macro-tiles goes to 0 as $N \to \infty$.

Non-linear Polynomial Stability

Theorem [Gayral and Sablik, 2021, Proposition 7.8 and Theorem 7.9]

For any $\varepsilon > 0$, any scale N, and any measure $\mu = \pi_1^*(\lambda)$ with $\lambda \in \widetilde{\mathcal{M}_{\mathcal{F}}^{\mathcal{B}}}(\varepsilon)$:

$$d_B\left(\mu, \mathcal{M}_{\mathcal{F}}\right) \leq 96\left(2^{N+2}+1\right)^2 \varepsilon + \frac{1}{2^{N-1}}.$$

Hence, the SFT is f-stable with $f(\varepsilon) = 48\sqrt[3]{6\varepsilon}$.

Aperiodic Instability

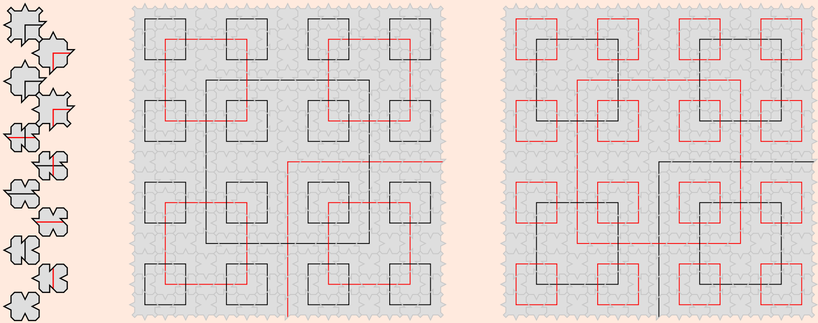

Figure 26: Two-coloured Robinson structure.

Proposition [Gayral, 2021, Proposition 1]

The SFT Ω_{RB} is unstable.

More precisely, for any $\varepsilon > 0$, we have $\mu \in \mathcal{M}^{\mathcal{B}}_{RB}(\varepsilon)$ such that $d_B(\mu, \mathcal{M}_{RB}) \geq \frac{1}{8}$.

Undecidability

We can embed Turing machines space-time diagrams into the Robinson structure.

Theorem [Gayral, 2021, Corollary 1]

The problem of deciding whether the SFT $\Omega_{\mathcal{F}}$ is stable or not given the set of forbidden patterns $\mathcal{F}$ is undecidable.

Random Dimers with Holes

What Happens to Dimers With the Besicovitch Distance?

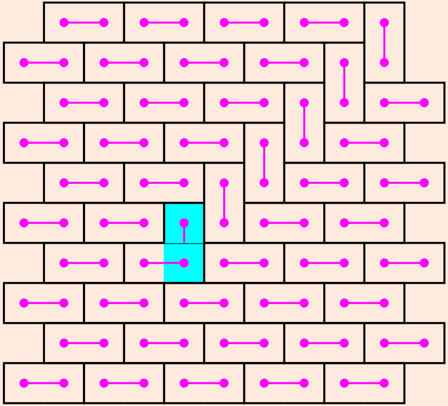

Figure 27: Example of a Domino SFT configuration, with one forbidden pattern highlighted in blue.

Bibliography

Luca Bindi et al.
Natural quasicrystal with decagonal symmetry.
Scientific reports, 5(1):1–5, 2015.

Léo Gayral and Mathieu Sablik.
On the Besicovitch-stability of noisy random tilings.
arxiv.org/abs/2104.09885v2, 2021.

Léo Gayral.
The Besicovitch-stability of noisy tilings is undecidable.
hal.archives-ouvertes.fr/hal-03233596, 2021.

THE END OF PRESENTATION

ONE MORE SLIDE:

Thank you.

Appendix 1: Computations for the Peierls Argument

Theorem

We have $\mathbb{E}_\beta[T] \leq \exp\left(\frac{9e^{2\beta}}{2(e^\beta+2)^2} \times \frac{1}{(e^\beta-2)^2}\right) - 1 < \infty$ *when* $\beta > \ln(2)$.

Proof.

We have:

$$
\begin{aligned}
\mathbb{P}(T(u) \geq k) &\leq \frac{1}{Z_{\Lambda,\beta}} \sum_{u \lhd \gamma_1 \lhd \cdots \lhd \gamma_k} \sum_{\eta \text{ compatible}} e^{-\beta E(\eta)} \\
&\leq \sum_{u \lhd \gamma_1 \lhd \cdots \lhd \gamma_k} \prod_{i=1}^{k} e^{-\beta|\gamma_i|} \times \left(\frac{1}{Z_\beta} \sum_{\eta \text{ compatible}} e^{-\beta E(\eta')}\right) \\
&\leq \sum_{u \lhd \gamma_1 \lhd \cdots \lhd \gamma_k} \prod_{i=1}^{k} e^{-\beta|\gamma_i|} \\
&\leq \frac{1}{k!} \left(\sum_{u \lhd \gamma} e^{-\beta|\gamma|}\right)^k .
\end{aligned}
$$

Appendix 1: Computations for the Peierls Argument

Theorem

We have $\mathbb{E}_\beta[T] \leq \exp\left(\frac{9e^{2\beta}}{2(e^\beta+2)^2} \times \frac{1}{(e^\beta-2)^2}\right) - 1 < \infty$ *when* $\beta > \ln(2)$.

Proof.

Thus:

$$\mathbb{E}[T(u)] \leq \exp\left(\sum_{u \triangleleft \gamma} e^{-\beta|\gamma|}\right) - 1\,.$$

Notice that:

$$\sum_{0 \triangleleft \gamma} e^{-\beta|\gamma|} \leq \sum_{\substack{k \geq 6 \\ k \in 2\mathbb{N}}} \frac{3}{8} k \times 3 \times 2^{k-1} \times e^{-\beta k} = \frac{9}{8} \sum_{l \geq 3} l \left(\frac{4}{e^{2\beta}}\right)^l\,.$$

This series is convergent as soon as $\frac{4}{e^{2\beta}} < 1$, *i.e.* $\beta > \ln(2)$, and the bound follows. $\square$